POLYPYRROLE SYNTHESIS VIA CARBOXYMETHYLCELLULOSE-IRON COMPLEXES

Claudia Sasso,[a,b] Davide Beneventi,[a] Elisa Zeno,[b,*] Didier Chaussy,[a] Michel Petit-Conil,[b] Patrice Nortier,[a] and Naceur Belgacem [a]

Polypyrrole (PPy) was chemically synthesised at two pH levels (pH = 2 and unadjusted pH, i.e. 6.6) using pre-formed carboxymethylcellulose-iron (CMC-Fe) complexes. The CMC-Fe complexes were prepared at a fixed CMC concentration, i.e. $5.5x10^{-5}$ mol/L, and with an increasing $FeCl_3$ amount (from $4x10^{-3}$ to $5x10^{-2}$ mol/L). The quantity of iron bound to CMC was determined by the inductively coupled plasma (ICP-MS) method. In order to understand the interactions between CMC and iron, speciation of the systems was simulated by Phreeqc software. SEM analysis showed that, in some conditions (particularly at pH = 2), Py polymerised within the CMC-Fe complexes, forming particles with size ranging between 300 and 600 nm. In order to evaluate polymer electric conductivity, films were prepared by direct casting of the PPy-CMC-Fe dispersions with and without addition of film-forming CMC, and bulky PPy-CMC-Fe pellets were obtained by compression. Despite the different arrangement PPy-CMC-Fe particles in dry films, the amount of iron bound to CMC during the formation of CMC-Fe complexes was found to be the dominant parameter affecting polymer conductivity.

Keywords: Carboxymethyl cellulose; Polypyrrole; Iron speciation; Complexes

Contact information: a: LGP2, UMR 5518 CNRS-Grenoble-INP, 461 rue de la Papeterie, Domaine Universitaire, BP 65, 38402 St. Martin d'Hères , France ; b : Centre Technique du Papier, Domaine Universitaire, BP. 251, 38044 Grenoble CEDEX 9, France
**Corresponding author: elisa.zeno@webCTP.com*

INTRODUCTION

Despite its environmental stability, good conductivity and the relative ease of synthesis, large-scale application of polypyrrole (PPy) has been impeded by the difficulties and limitations associated with its processing. In fact, PPy cannot be dissolved or melted. In this context, PPy dispersions represent a possible solution to avoid such a drawback. Thus, colloidal PPy synthesis has been widely investigated, and stable PPy dispersions with particle size ranging between 20 and 700 nm have been obtained by adding, in the pyrrole (Py) polymerisation liquor, polymeric stabilizers such as 2-(dimethylamino)ethyl methacrylate (Martin 1995; Simmons et al. 1998; Simmons et al. 1995), polyvinyl alcohol (Armes et al. 1987; Men'shikova et al. 2003), azobenzenesulfonic acid (Antony and Jayakannan 2009), and poly(2-vinyl pyridine-co-butyl methacrylate) (Armes and Aldissi 1990). Other methods to produce nanosized PPy involve, for example, the realisation of core-shell structures in which PPy encapsulates polystyrene latexes (Cho et al. 2005; Lascelles et al. 1997; Lascelles and Armes 1995), or the synthesis of PPy-silica nano-composites (Lascelles and McCarthy 1998; Maeda and Armes 1994; Han et Armes 2003). PPy particles with nano-dimensions, but with a less

controlled shape can be produced by using surfactants during polymerisation (Qi and Pickup 1997; DeArmitt and Armes 1993; Kudoh 1996; Xing et Zhao 2007). Wood derivatives, such as methylcellulose (Bjorklund and Liedberg 1986), carboxymethyl-cellulose (CMC) (Sasso et al. 2007), ethylhydroxy-ethylcellulose (Mandal and Mandal 1995, 1999), and hydroxypropylcellulose (Amaike and Yamamoto 2006) have been also used to prepare colloidal PPy with particle size ranging from 20 to 200 nm. Particularly, it was found that PPy particle size was affected by the additive and/or the oxidant concentration (Mandal and Mandal 1995; Amaike and Yamamoto 2006).

Py chemical synthesis is often carried out using $FeCl_3$ as oxidant and an anionic polyelectrolyte, often referred as doping agent. Most of the time, $FeCl_3$ and the polyelectrolyte are mixed before monomer addition with the subsequent formation of polyelectrolyte-iron complexes with iron depletion from the aqueous solution. Despite this recurrent phenomenon during PPy synthesis, the role of polyelectrolyte-iron complexes, and in particular CMC-iron complexes, remains rather unexplored.

The formation of complexes between biopolymers and metals is known in different industrial applications such as wastewater bio-cleaning and metal ions tracing (Houghton and Quarmby 1999; Chen et al. 2000). In these processes, cellulose derivatives (such as CMC) are widely used because of their selective affinity with heavy metal ions. Even if some studies on the chelates of metals (such as aluminium, vanadium, lead, molybdenum) with cellulose derivatives have been carried out (Franco et Mercê 2006; Franco et al. 2007), to the best of our knowledge, CMC-iron complexes have been insufficiently investigated (Basta et El-Saied 2000; Hosny et al. 1997).

In aqueous solutions, $FeCl_3$ hydrolysis leads to the formation of both aquo-hydroxo complexes between iron, chloride ions and water such as: $Fe(H_2O)_6^{3+}$, $Fe(H_2O)_5(OH)^{2+}$, $Fe(H_2O)_4(OH)_2^{+}$, and $Fe(H_2O)_3(OH)_3^{0}$ for hexa-coordinated aquo complexes (Baes and Mesmer 1986; Jolivet et al. 2004; Flinn 1984) and $[Fe_xO_y(OH)_zCl_u{\cdot}nH_2O]^{+}$ and $[Fe_aO_b(OH)_cCl_d{\cdot}nH_2O]^{-}$ for chloride-containing complexes (Hellmann et al. 2006; Beneventi et al. 2006). Owing to their cationic charge, most of the iron-containing species are susceptible to react with CMC. Nevertheless, according to Hosny et al. (1997) CMC-Fe (III) chelates exhibit a brown colour and can be described by a single general chemical formula: $[(CMC)FeCl{\cdot}H_2O]Cl{\cdot}2H_2O$. In this paper an attempt to obtain size-controlled PPy dispersion based on pyrrole polymerisation in the presence of CMC-Fe complexes is presented. The objective of this approach was to use CMC-Fe complexes as size-limited structures in which pyrrole could grow (Fig. 1.b).

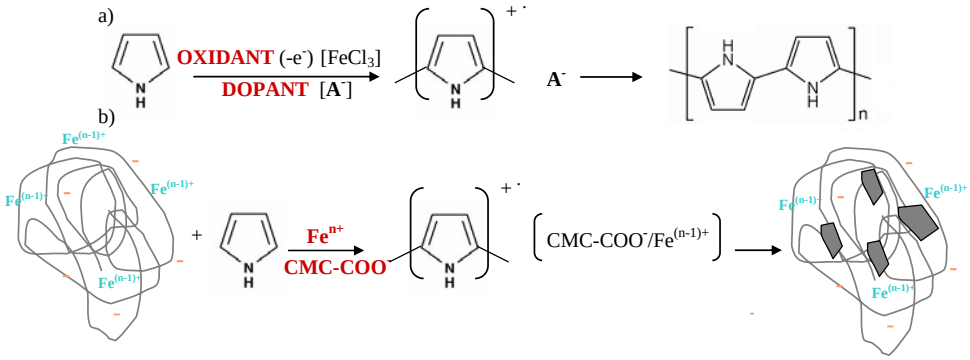

Fig. 1. Pyrrole polymerisation: a) by classical chemical oxido-reduction; b) hypothetical representation of PPy polymerisation *via* CMC-Fe^{n+} complexes formation

Pyrrole polymerisation would therefore proceed because electron acceptor and electron donor moieties in the CMC-Fe complexes are supposed to act as an oxidant and as a dopant, respectively. Moreover, the insertion of PPy particles within a CMC-based coil could favour film formation, creating a network among PPy-CMC-Fe particles.

EXPERIMENTAL

Materials

Pyrrole (Aldrich) was distilled under vacuum and stored at 4°C before use. $FeCl_3$ (Aldrich) and carboxymethyl cellulose (DS 0.7, MW 250000, Aldrich) were used as received. HCl served to adjust the solutions' pH.

Methods

CMC-Fe complex formation and pyrrole polymerisation

Na-CMC ($5.5x10^{-5}$ mol/L) and $FeCl_3$ (concentrations reported in Table 1) were dissolved in deionised water at pH = 2 (pH adjusted by HCl addition) and unadjusted pH. $FeCl_3$ and CMC solutions were then mixed, and CMC-Fe complex dispersions were left under magnetic stirring overnight. Dispersions turbidity was then measured (2100 P, Hach) and three cycles of centrifugation were carried out (15 minutes, 10000 rpm) in order to eliminate free iron cations (those not bond to CMC macromolecules). The recovered solid phase, supposed to contain essentially CMC-Fe complex, was poured into water (at the corresponding initial pH) and dispersed by ultrasonication. Pyrrole was then added with a ratio Fe^{3+}/Py=2.33 (w/w) (Armes et al. 1987; Men'shikova et al. 2003) with respect to the initial iron concentration. After overnight (17 h) polymerisation under magnetic stirring, PPy particles were washed with deionised water (3 cycles of centrifugation of 15 minutes at 10000 rpm), collected, and dispersed again in an equal volume of water by ultrasonication. The resulting PPy-CMC-Fe particle size distribution was evaluated by Dynamic Light Scattering (Zeta Sizer NanoZS, Malvern). SEM (Scanning Electron Microscopy) (Fei Quanta 200) and FE-SEM (Zeiss Ultra 55) examinations were also performed for a selection of several samples (A2, B2, C2, A6.6, B6.6 and C6.6, see Table 1).

Table 1. Experimental Conditions Used for the Formation of the Complexes

pH	Na-CMC Concentration [mol/L]	$FeCl_3$ concentration [mol/L]	Reference
2	$5.5x10^{-5}$	$2.0x10^{-3}$	
		$4.0x10^{-3}$	A2
		$1.0x10^{-2}$	
		$2.5x10^{-2}$	B2
		$5.0x10^{-2}$	C2
6.6	$5.5x10^{-5}$	$2.0x10^{-3}$	
		$4.0x10^{-3}$	A6.6
		$1.0x10^{-2}$	
		$2.5x10^{-2}$	B6.6
		$5.0x10^{-2}$	C6.6

The formation of the different species formed after mixing CMC and $FeCl_3$ was simulated with Phreeqc software (Parkhurst and Appelo 1999) for the samples A2, B2, C2, A6.6, B6.6, and C6.6 (Table 1).

The complex considered was $[(CMC)FeCl{\cdot}H_2O]Cl{\cdot}2H_2O$ (Hosny et al. 1997). The original database delivered by in Phreeqc distribution was modified by adding the following formation constants:

- $CMC^- + H^+ = HCMC$ logk = 3 (Franco and Mercê 2006)
- $CMC^- + Na^+ = NaCMC$ logk = 1
- $CMC^- + Fe^{3+} + Cl^- = CMCFeCl^+$ logk = 5.505 (Hosny et al. 1997)
- $FeO(OH) + 3H^+ = Fe^{3+} + 2H_2O$ logk = 4 (Baes and Mesmer 1986)

The average equivalent CMC molecular weight, for which a carboxylic unit was found, was calculated (from the degree of substitution of the CMC = 0.7) as 300 g/mol. A sample input for Phreeqc is presented in the annex section.

The free iron remaining in the liquid phase after CMC-Fe complexes separation by centrifugation was measured by inductively coupled plasma mass spectrometry (Perkin Elmer, ICP-MS Elan DRC) after 100-1000 times sample dilution (depending on the initial $FeCl_3$ concentration) with deionised water and acidification to pH 2 with HNO_3. The quantity of iron in CMC-Fe complexes was calculated as the difference between the initial introduced iron and the measured free iron. This technique did not permit discrimination of the different types of bonds (electrostatic, chemical, physical, etc.) between CMC and iron.

Film formation

Films were formed by direct casting of polymerisation dispersions (in this case, films were obtained only for the samples obtained at pH = 6.6), or by addition of a film-forming agent (50 g/L CMC solution) to the PPy-CMC-Fe particle suspension.

Films were cast on a Teflon mould (Fig. 2), and left drying overnight. The electrical properties were determined with the four-probe test (Jandel, Universal Probe).

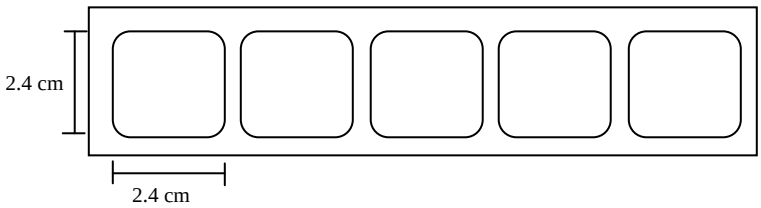

Fig. 2. Scheme of the Teflon® mould used to obtain films

RESULTS AND DISCUSSION

CMC-Fe Complex Formation and Pyrrole Polymerisation

Fig. 3 shows PPy dispersions after polymerisation at different pH and $FeCl_3$ concentration. Most of the samples showed a dark-black colour (B2, C2, B6.6, C6.6), while A samples were lighter, because they were obtained at low initial $FeCl_3$ concentration, A2 was green-black, and A6.6 was light orange.

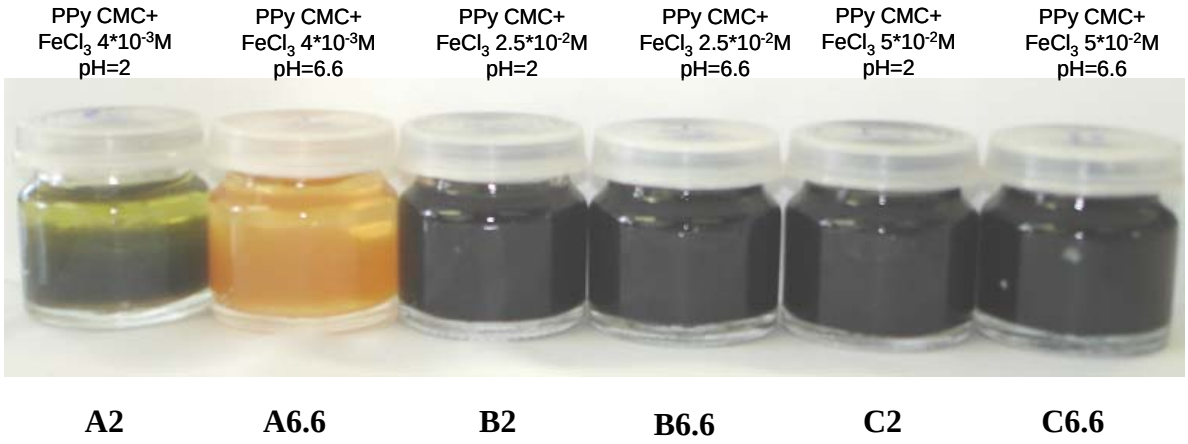

Fig. 3. PPy polymerisation baths in the presence of: A2) [$FeCl_3$]= $4x10^{-3}$ mol/L and [CMC]= $5.5x10^{-5}$ mol/L, pH=2; A6.6) [$FeCl_3$]= $4x10^{-3}$ mol/L and [CMC]= $5.5x10^{-5}$ mol/L, pH=6.6; B2) [$FeCl_3$]= $2.5x10^{-2}$ mol/L and [CMC]= $5.55x10^{-5}$ mol/L, pH=2; B6.6) [$FeCl_3$]= $2.5x10^{-2}$ mol/L and [CMC]= $5.5x10^{-5}$ mol/L, pH=6.6; C2) [$FeCl_3$]= $5x10^{-2}$ mol/L and [CMC]= $5.5x10^{-5}$ mol/L, pH=2; C6.6) [$FeCl_3$]= $5x10^{-2}$ mol/L and [CMC]= $5.5x10^{-5}$ mol/L, pH=6.6.

As the colour of the dispersion can be associated with the extent of polymerisation (complete polymerisation gives black dispersions), it could be assumed that the polymerisation was incomplete, particularly for the A6.6 sample. To evaluate the complex formation with respect to (initial) pH, iron, and CMC speciation was computed with Phreeqc software (see Fig. A.1-3 in the annex section). The CMC-Fe complex concentration *versus* the final pH (Fig. 4) shows that, when increasing the initial $FeCl_3$ concentration, the amount of CMC-Fe complex increases too. This was interpreted as reflecting the presence of a strong excess of CMC, with respect to the CMC/Fe interaction, for all tested conditions. For conditions B (initial [$FeCl_3$]=$2.5x10^{-2}$ mol/L) and C (initial [$FeCl_3$]=$5x10^{-2}$ mol/L), model calculations predicted the formation of similar amounts of CMC-Fe whatever the initial pH. This similarity was associated with the strong acidic behavior of iron chloride which, at sufficiently high concentration, i.e. [$FeCl_3$] > $2x10^{-2}$ mol/L, lowers the pH of water-$FeCl_3$ solutions below 2 (Beneventi et al. 2006). In these conditions, the presence of HCl used to adjust the initial pH to 2, slightly affected the pH of CMC-$FeCl_3$ solutions which ranged between 1.5 and 2. Fig. 4 shows that, at high $FeCl_3$ concentration (2.5 and $5x10^{-2}$ mol/L), the pH decrease from 2 to 1.5 due to the presence of HCl induced a negligible variation in the CMC-Fe concentration. By contrast, at low $FeCl_3$ concentration ($4x10^{-3}$ mol/L) and in the absence of HCl, CMC-$FeCl_3$ solutions had pH ca. 3, and aquo-hydroxo complexes formed at the expenses of Fe^{3+} (Fig. A.1) and of the CMC-Fe complex. Trends given by model calculations are in line with the absence of PPy polymerisation in the A6.6 sample. The amount of iron present in CMC-Fe complexes, as determined from free iron dosage by ICP-MS, was in line with trends obtained from both visual examinations and Phreeqc simulations.

Moreover, pH would affect the solution redox potential. Michalska and Maksymiuk (1998) reported that a low pH would increase the redox potential, thus favouring monomer oxidation and enhancing polymerisation.

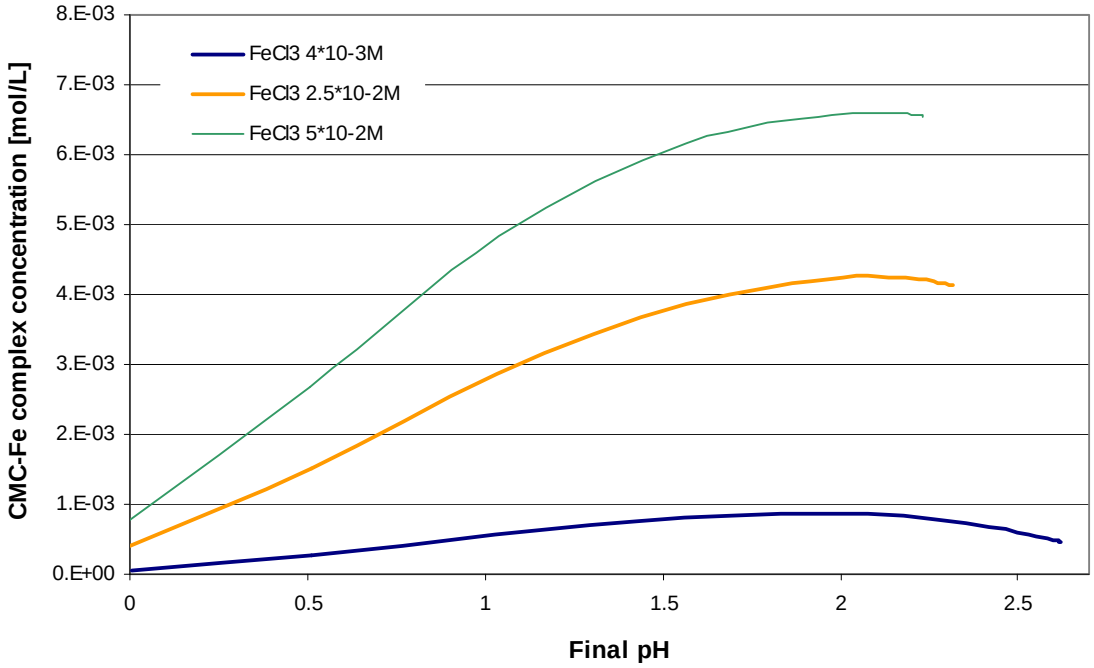

Fig. 4. CMC-Fe complex concentration obtained with Phreeqc as a function of final pH and different initial $FeCl_3$ concentration

At low pH, the iron involved in the CMC-Fe complex formation was supposed to maintain an oxidation potential high enough to initiate pyrrole polymerisation. However at high pH, iron cationic species tended to interact with both the deprotonated CMC ($CMC\text{-}COO^-$), forming a cross-linked network, and hydroxide moieties (annex Fig A.1), thus lowering iron oxidation potential.

From the comparison of experimental and simulated values (Table 2), it can be pointed out that bond iron computed values were generally underestimated when compared with experimental data, particularly at initial pH = 6.6. This mismatch could be attributed to the fact that the simulation did not take into account the possible reactions between the negatively charged carboxylic groups of CMC ($CMC\text{-}COO^-$) and other iron cationic species, such as $FeCl^{2+}$, $FeCl_2^+$, $FeOH_2^+$, and $FeOH^{2+}$. Such a limitation induced the underestimation of the final iron content, particularly at pH = 6.6 where $CMC\text{-}COO^-$ was more concentrated. Morphological analysis of air-dried PPy particles (obtained at an initial $FeCl_3$ concentration of $4x10^{-3}$ mol/L, pH = 2 and pH = 6.6) were carried out by FE-SEM (Fig. 5).

At low pH, individual vesicle-like particles were observed (Fig. 5 a-c), while at high pH, a continuous network was detected (Fig. 5 d-f). This was associated with the different tendency of the two systems to form cross-linked networks. At pH = 2, the high amount of protonated CMC (HCMC) impeded the coordination of several CMC macromolecules by iron cationic species. However at pH = 6.6 a cross-linked network of CMC and iron easily formed.

Table 2. Theoretical and Experimental Amounts of Bound Iron *

Initial $FeCl_3$ concentration [mol/L]	Initial Fe concentration [mg/L]	Fe in CMC-$Fe_{initial\ pH=2}$ [mg/L]	Fe in CMC-$Fe_{initial\ pH=6.6}$ [mg/L]	Calculated Fe in CMC-$Fe_{initial\ pH=2}$ [mg/L]	Calculated Fe in CMC-$Fe_{initial\ pH=6.6}$ [mg/L]
$4.0x10^{-3}$	223	68.2	147.5	62.2	34.5
$2.5x10^{-2}$	1400	155.7	600.3	310.1	301.8
$5.0x10^{-2}$	2790	918.9	1064.8	480.5	478.6

* Iron amount in complexes was calculated according to the iron percentage in complexes established by Hosny (15.2 %).

Micrographs taken at higher magnification (Fig. 5 b-c) revealed that vesicles obtained at low pH were composed of a smooth continuous phase, which was associated with CMC, and small particles with cauliflower aspect typical of chemically synthesised PPy. The presence of two distinct phases was interpreted as reflecting only the partial polymerisation of Py with CMC-Fe complexes. At pH = 6.6, PPy particles were not clearly detectable because of their low (or negligible) concentration, and the irregular surface shown in Fig. 5 e-f was attributed to the formation of a crackled film of CMC-Fe complexes.

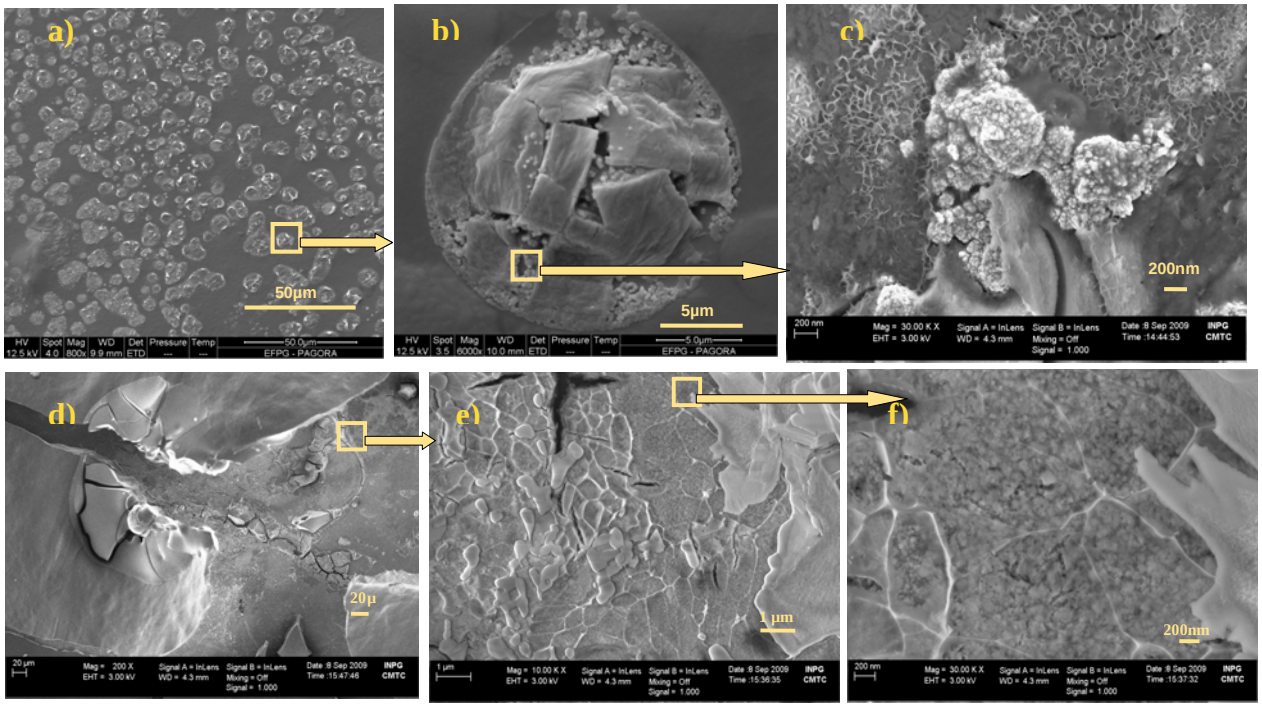

Fig. 5. PPy-FeCMC particle morphology, obtained from pH = 2 (a, b, c) and pH = 6.6 (d, e, f). Complexes were realized starting from [$FeCl_3$] = $4x10^{-3}$ mol/L.

Results observed with electron microscopy concerning the physical organisation of PPy-CMC-Fe particles were confirmed by dynamic light scattering analysis (Fig. 6). Due to the lower CMC cross-linking ability of iron cations at low pH, PPy-CMC-Fe particles had smaller size (300-600 nm) than those obtained at high pH (400-4000 nm).

Moreover, when increasing $FeCl_3$ concentration (from $4x10^{-3}$ to $2.5x10^{-2}$ mol/L) at high pH, the PPy-CMC-Fe particle size increased by more than one order of magnitude. This was attributed to the formation of larger PPy-CMC-Fe particle networks with a higher $FeCl_3$ initial concentration. However, $FeCl_3$ concentration had a slight influence on the size of particles obtained at initial pH = 2.

The effect of pH on PPy-CMC-Fe particles size was in line with the turbidity of CMC-Fe dispersions before Py addition, i.e. 56 and 30 NTU ($4x10^{-4}$ mol/L $FeCl_3$) at initial pH 2 and 6, respectively. Owing to the presence of a constant concentration of CMC, the low turbidity value obtained at initial pH 6 was attributed to the formation of large CMC-Fe complexes, and the high turbidity of the acidic dispersion to the formation of finely dispersed complexes.

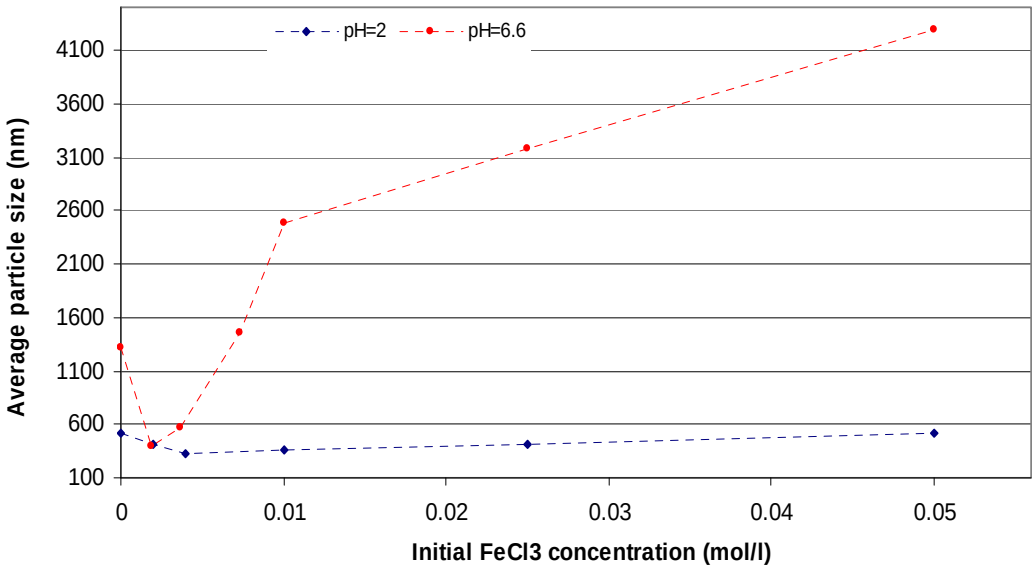

Fig. 6. PPy particle size obtained at different initial pH and increasing $FeCl_3$ concentration

Figure 7 shows the conductivity of CMC-Fe-PPy pellets as a function of $FeCl_3$ concentration and initial pH. Generally, conductivity increased when increasing $FeCl_3$ (i.e. bond iron) concentration, and particles synthesised at higher pH displayed higher conductivity. This trend was attributed to the different amount of iron present in CMC-Fe complexes (inset in Fig. 7). CMC-Fe complexes obtained with initial pH 2 and $2.5x10^{-2}$ mol/L of $FeCl_3$, and with initial pH 6 and $4x10^{-3}$ mol/L of $FeCl_3$, had similar low iron content (Table 2), which limited Py polymerisation, and the conductivity of the corresponding CMC-Fe-PPy pellets, which were completely resistive. At the highest $FeCl_3$ concentration, CMC-Fe complexes had similar high iron content for the two initial pH values, which led to comparable extent of Py polymerisation and CMC-Fe-PPy pellet conductivity.

Films were cast from both PPy dispersions or after the addition of CMC (50 g/L solution). While films obtained with the former method were not continuous, those produced with the latter were homogeneous, and their conductivity ranged from 10^{-3} to 10^{-2} S/cm, depending on the amount of non conducting CMC added to the CMC-Fe-PPy dispersion.

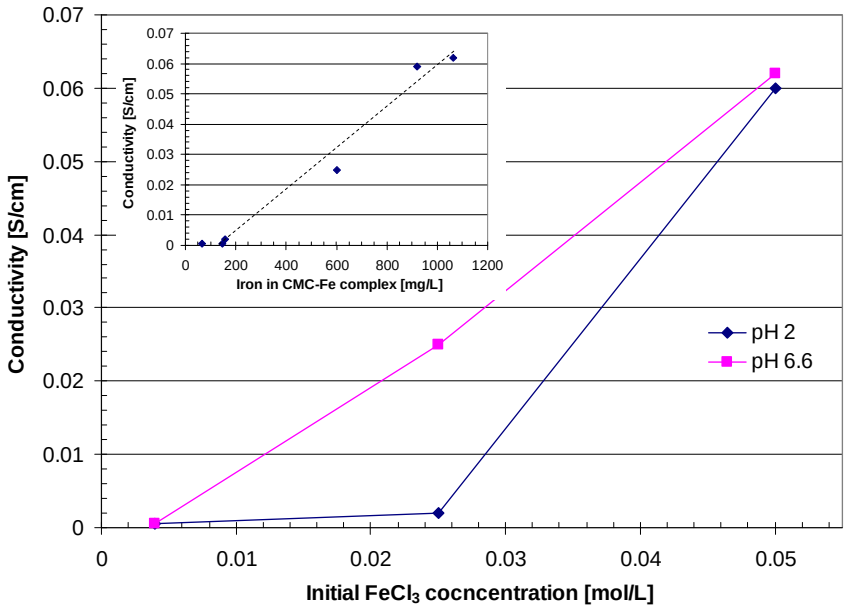

Fig. 7. PPy pellet conductivity. PPy was synthesised with CMC-Fe complexes obtained at initial [CMC] = $5.55x10^{-5}$ mol/L and [$FeCl_3$] = $4x10^{-3}$ mol/L, $2.5x10^{-2}$ mol/L; $5x10^{-2}$ mol/L. Inset represents PPy pleet conductivity plotted as a function of iron amount in CMC-Fe complex (as determined by ICP-MS).

CONCLUSIONS

The following general conclusions can be drawn from this investigation.

1. Simulation of iron and CMC speciation using Phreeqc software and formation constants given in the literature provided a qualitative evaluation of iron present in CMC-Fe complexes. Indeed, simulated values were lower than measured ones, indicating that the considered complexation mechanisms were not sufficient to properly describe the formation of CMC-Fe. CMC reaction with iron cationic species, such as $FeCl^{2+}$, $FeCl_2^{+}$, $FeOH_2^{+}$ and $FeOH^{2+}$ were supposed to be at the origin of this mismatch; however the unavailability of reaction constants did not allow the running of simulations. Additional experimental work would be required for the complete determination of iron and CMC speciation and the corresponding formation constants.
2. Initial pH and $FeCl_3$ concentration influenced PPy polymerisation. At low pH, protonated CMC did not form a crosslinked network with iron cations, and final PPy particles had size ranging between 300 and 600 nm. At pH 6, deprotonated CMC formed a crosslinked network with iron cations which, despite ultrasonication, induced the formation of large PPy particles (400-4000 nm). Moreover, CMC deprotonation at high pH improved CMC-iron electrostatic interactions, the amount of iron present in the CMC-Fe complex, the extent of Py polymerisation and, finally, PPy pellets conductivity. In the presence of a strong excess of $FeCl_3$, pH had a negligible effect of the amount of iron bond to CMC and pellet conductivity.

3. Continuous films were obtained by direct PPy-CMC-Fe casting only for particles produced at pH = 6.6. But, in this case, conductivity was variable. With the addition of supplementary CMC, conductivity slightly decreased but smooth-regular films were obtained. Work is in progress to overcome these limitations and to evaluate the use of PPy-CMC-Fe particles in the formulation of conductive inks/coatings.

ACKNOWLEDGEMENT

This work was supported by a CIFRE grant from the French "Association Nationale de la Recherche et de la Technologie," and by CTP and CTPi members.

REFERENCES CITED

Amaike, M., and Yamamoto, H. (2006). "Preparation of polypyrrole by emulsion polymerization using hydroxypropyl cellulose," *Polym. J.* 38, 703-709.

Antony, M. J., and Jayakannan, M. (2009). "Self-assembled anionic micellar template for polypyrrole, polyaniline, and their random copolymer nanomaterials," *Journal of Polymer Science Part B: Polymer Physics* 47, 830-846.

Armes, S., and Aldissi, M. (1990). "Preparation and characterization of colloidal dispersions of polypyrrole using poly(2-vinyl pyridine)-based steric stabilizers," *Polymer* 31, 569-574.

Armes, S. P., Miller, J. F., and Vincent, B. (1987). "Aqueous dispersions of electrically conducting monodisperse polypyrrole particles," *Journal of Colloid and Interface Science* 118, 410-416.

Baes, C. F., and Mesmer, R. E. (1986). *The Hydrolysis of Cations*, Krieger, R. E. (ed.), Wiley.

Basta, A. H., and El-Saied, H. (2000). "Characterisation of polymer complexes by thermal and IR spectral analyses," *Polymer-Plastics Technology and Engineering* 39, 887-904.

Beneventi, D., Alila, S., Boufi, S., Chaussy, D., and Nortier, P. (2006). "Polymerization of pyrrole on cellulose fibres using a FeCl3 impregnation- pyrrole polymerization sequence," *Cellulose* 13, 725-734.

Bjorklund, R., and Liedberg, B. (1986). "Electrically conducting composites of colloidal polypyrrole and methylcellulose," *Journal of the Chemical Society. Chemical communications* 16, 1293-1295.

Chen, L. A., Carbonell, R. G., and Serad, G. A. (2000). "Recovery of proteins and other biological compounds from food processing wastewaters using fibrous materials and polyelectrolytes," *Water Research* 34, 510-518.

Cho, S., Kim, W., Jeong, G., and Lee, Y. (2005). "Synthesis of nano-sized polypyrrole-coated polystyrene latexes," *Colloids and Surfaces A: Physicochemical and Engineering Aspects* 255, 79-83.

DeArmitt, C., and Armes, S. P. (1993). "Colloidal dispersions of surfactant-stabilized polypyrrole particles," *Langmuir* 9, 652-654.

Flynn, C. M. (1984). "Hydrolysis of inorganic iron(III) salts," *Chemical Reviews* 84, 31-41.

Franco, A. P., and Mercê, A. L. R. (2006). "Complexes of carboxymethylcellulose in water. 1: Cu^{2+}, VO^{2+} and Mo^{6+}," *Reactive and Functional Polymers* 66, 667-681.

Franco, A. P., Recio, M. A. L., Szpoganicz, B., Delgado, A. L., Felcman, J., and Mercê, A. L. R. (2007). "Complexes of carboxymethylcellulose in water. Part 2. Co^{2+} and Al^{3+} remediation studies of wastewaters with Co^{2+}, Al^{3+}, Cu^{2+}, VO^{2+} and Mo^{6+}," *Hydrometallurgy* 87, 178-189.

Han, M. G., and Armes, S. P. (2003). "Preparation and characterization of polypyrrole-silica colloidal nanocomposites in water-methanol mixtures," *Journal of Colloid and Interface Science* 262, 418-427.

Hellman, H., Laitinen, R. S., Kaila, L., Jalonen, J., Hietapelto, V., Jokela, J., Sarpola, A., and Rämö, J. (2006). "Identification of hydrolysis products of $FeCl_3 \cdot 6H_2O$ by ESI-MS," *Journal of Mass Spectrometry* 41, 1421-1429.

Hosny, W. M., Basta, A. H., and El-Saied, H. (1997). "Metal chelates with some cellulose derivatives: V. Synthesis and characterization of some iron(III) complexes with cellulose ethers," *Polymer International* 42, 157-162.

Houghton, J. I., and Quarmby, J. (1999). "Biopolymers in wastewater treatment," *Current Opinion in Biotechnology* 10, 259-262.

Jolivet, J., Chaneac, C., and Tronc, E. (2004). "Iron oxide chemistry. From molecular clusters to extended solid networks," *Chemical Communications* 5, 481-487.

Kudoh, Y. (1996). "Properties of polypyrrole prepared by chemical polymerization using aqueous solution containing $Fe_2(SO_4)_3$ and anionic surfactant," *Synthetic Metals* 79, 17-22.

Lascelles, S. F., and Armes, S. P. (1995). "Synthesis and characterization of micrometersized polypyrrole-coated polystyrene latexes," *Advanced Materials* 7, 864-866.

Lascelles, S. F., Armes, S. P., Zhdan, P. A., Greaves, S. J., Brown, A. M., Watts, J. F., Leadley, S. R., and Luk, S. Y. (1997). "Surface characterization of micrometre-sized, polypyrrole-coated polystyrene latexes: Verification of a 'core-shell' morphology," *Journal of Materials Chemistry* 7, 1349-1355.

Lascelles, S. F., McCarthy, G. P., Butterworth, M. D., and Armes, S. P. (1998). "Effect of synthesis parameters on the particle size, composition and colloid stability of polypyrrole–silica nanocomposite particles," *Colloid & Polymer Science* 276, 893-902.

Maeda, S., and Armes, S. P. (1994). "Preparation and characterisation of novel polypyrrole-silica colloidal nanocomposites," *Journal of Materials Chemistry* 4, 935-942.

Mandal, T. K., and Mandal, B. M. (1995). "Ethylhydroxyethylcellulose stabilized polypyrrole dispersions," *Polymer* 36, 1911-1913.

Mandal, T. K., and Mandal, B. M. (1999). "Dispersion polymerization of pyrrole using ethylhydroxy-ethylcellulose as a stabilizer," *Journal of Polymer Science Part A: Polymer Chemistry* 37, 3723-3729.

Martin, C. R. (1995). "Template synthesis of electronically conductive polymer nanostructures," *Accounts of Chemical Research* 28, 61-68.

Men'shikova, A., Shabsel's, B., and Evseeva, T. (2003). "Synthesis of polypyrrole nanoparticles by dispersion polymerization," *Russian Journal of Applied Chemistry* 76, 822-826.

Michalska, A., and Maksymiuk, K. (1998). "On the pH influence on electrochemical properties of poly(pyrrole) and poly(n-methylpyrrole)," *Electroanalysis* 10, 177-180.

Parkhurst, D. L. and Appelo, C. A. J. (1999). "User's guide to PHREEQC (version 2)--A computer program for speciation, batch-reaction, one-dimensional transport, and inverse geochemical calculations," U.S. Geological Survey Water-Resources Investigations Report 99-4259.

Qi, Z., and Pickup, P. G. (1997). "Size control of polypyrrole particles," *Chemistry of Materials* 9, 2934-2939.

Sasso, C., Beneventi, D., Zeno, E., Chaussy, D., Petit-Conil, M., and Belgacem, M. N. (2010). "Carboxymethyl cellulose in organic electronics: A dopant and film-forming agent for processable polypyrrole from aqueous medium," submitted for publication.

Simmons, M. R., Chaloner, P. A., and Armes, S. P. (1995). "Synthesis of colloidal polypyrrole particles using reactive polymeric stabilizers," *Langmuir* 11, 4222-4224.

Simmons, M. R., Chaloner, P. A., Armes, S. P., Greaves, S. J., and Watts, J. F. (1998). "Synthesis and characterization of colloidal polypyrrole particles using reactive polymeric stabilizers," *Langmuir* 14, 611-618.

Xing, S., and Zhao, G. (2007). "Morphology, structure, and conductivity of polypyrrole prepared in the presence of mixed surfactants in aqueous solutions," *Journal of Applied Polymer Science* 104, 1987-1996.

Article submitted: July 29, 2010; Peer review completed: Sept. 6, 2010; Revised version received and accepted: September 14, 2010; Published: September 16, 2010.

ANNEX

Example of the Phreeqc code used to compute iron and CMC speciation in water with $[FeCl_3] = 4x10^{-3}$ mol/L and [CMC]= $5.55x10^{-5}$ mol/L:

```
SOLUTION 1                    # initial solution at adjusted pH
        pH 2
        pe 14.8
        -units mol/L
        Cl      1       charge
End

USE SOLUTION 1                # Addition of CMC to the initial solution
REACTION 1
        CMC     1.67e-2
        Na      1.67e-2
SAVE SOLUTION 2
End
```

```
USE SOLUTION 1                  # Addition of FeCl3 to the initial solution
REACTION 2
        Fe 4e-3
        Cl 12e-3
SAVE SOLUTION 3
End

MIX 1                           # Mix of the solution containing FeCl3 and that one containing the CMC: complex formation
2 1
3 1
END
```

Complete speciation diagrams of CMC-$FeCl_3$ aqueous systems as obtained with Phreeqc simulations:

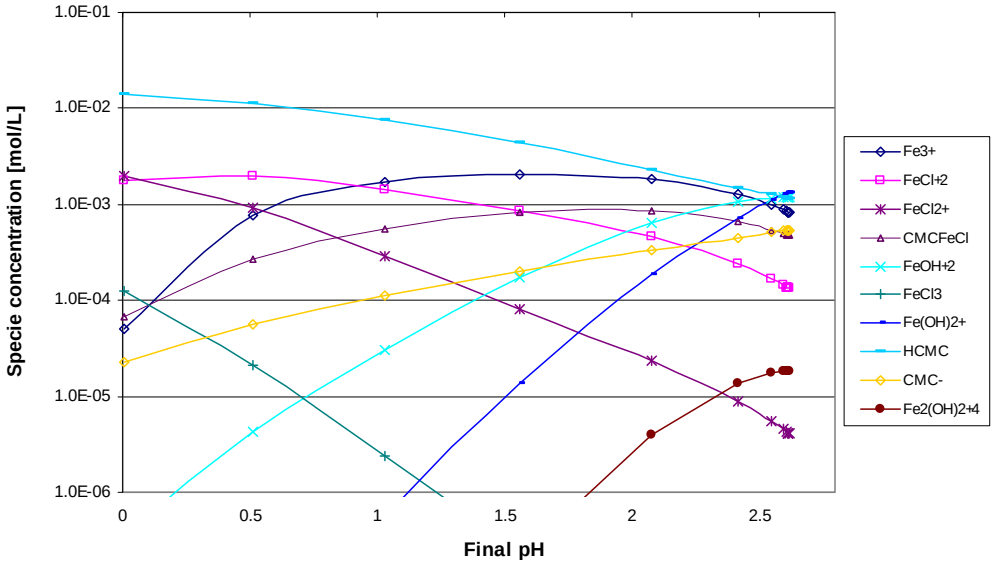

Fig. A.1. Speciation of $FeCl_3$ and CMC obtained with Phreeqc with [$FeCl_3$]= $4x10^{-3}$ mol/L and [CMC]= $5.5x10^{-5}$ mol/L

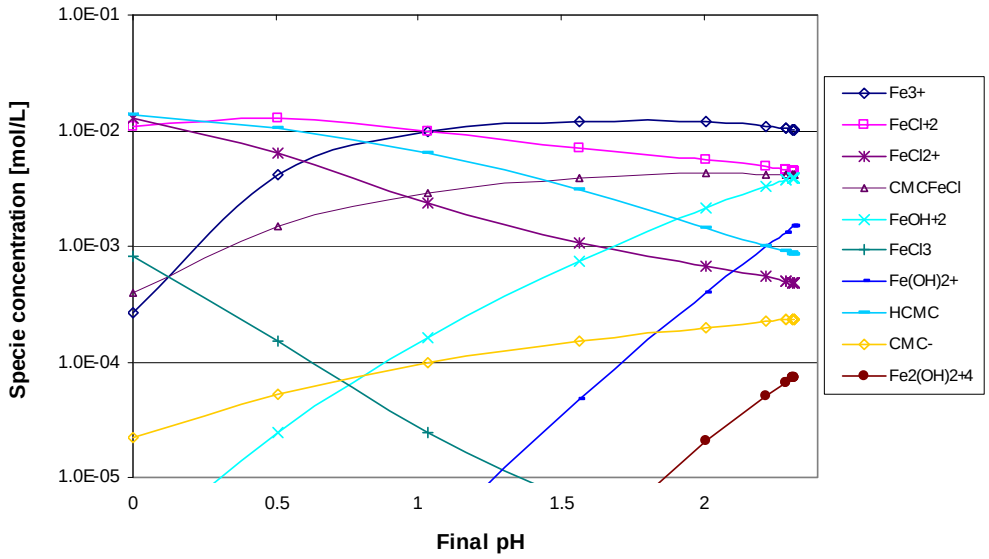

Fig. A.2 Speciation of $FeCl_3$ and CMC obtained with Phreeqc with [$FeCl_3$]= $2.5x10^{-2}$ mol/L and [CMC]= $5.5x10^{-5}$ mol/L

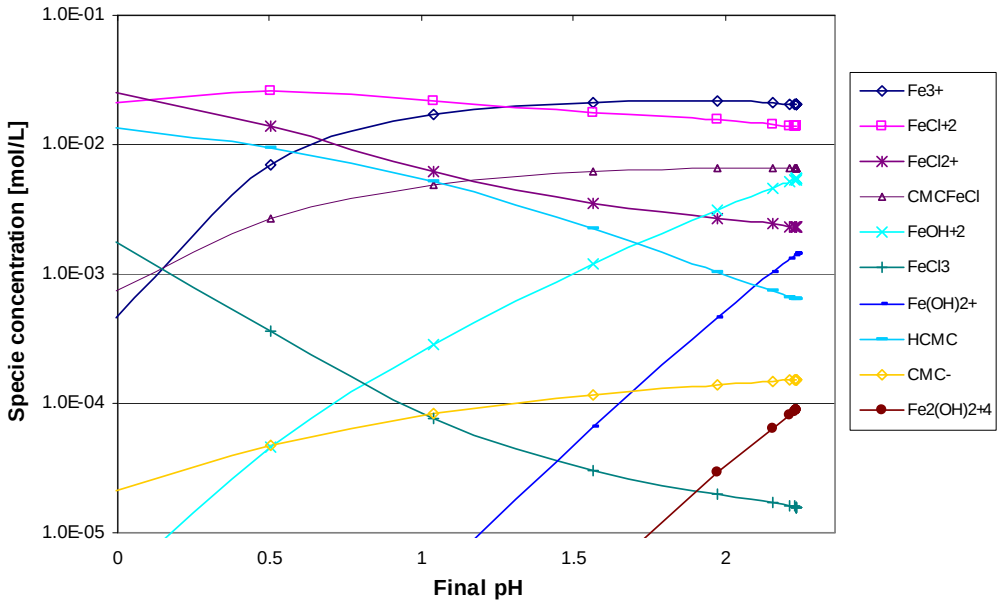

Fig. A.3 Speciation of $FeCl_3$ and CMC obtained with Phreeqc with [$FeCl_3$]= $5x10^{-2}$ mol/L and [CMC]= $5.5x10^{-5}$ mol/L